0254-6124/2014/34(3)-287–09 *Chin. J. Space Sci.* 空间科学学报

Yu Tao, Mao Tian, Xia Chunliang, Wan Weixing. A simulation of the mid- and low-latitude ionospheric electric fields. (in Chinese). *Chin. J. Space Sci.*, 2014, **34**(3): 287-295, doi:10.11728/cjss2014.03.287

A Simulation of the Mid- and Low-latitude Ionospheric Electric Fields

YU Tao[1] MAO Tian[1] XIA Chunliang[2] WAN Weixing[3]

1(*National Satellite Meteorological Center, China Meteorological Administration, Beijing* 100081)

2(*China University of Geosciences, Wuhan* 430074)

3(*Institute of Geology and Geophysics, Chinese Academy of Sciences, Beijing* 100029)

Abstract A theoretical model of ionospheric electric fields at mid- and low-latitudes is developed. In the geomagnetic dipolar coordinate system, the ionospheric dynamo equations were solved, and the ionospheric electric potential and electric field were derived respectively. Major parameters for the model inputs, such as the neutral winds, the densities and temperatures of electron, ions and neutrals, are obtained from empirical models. The global ionospheric electrical potential and field at mid- and low-latitudes derived from our model are largely in agreement with the results presented by other authors and the empirical model. Using our model, it is found that the diurnal component of the HWM93 wind mainly contributed to the formation of the vertical electric field, while the semidiurnal component mainly contributed to the zonal electric field. Finally, by adjustment of the input F region winds and conductivities, most discrepancies between our model and the empirical one can be eliminated, and it is proved that the F region dynamo is the most significant contribution to the electric fields.

Key words Ionosphere dynamo, Simulation, Tides, Zonal electric field evening enhancement

Classified Index P 352

0 Introduction

The electrodynamics processes in the ionosphere is of significant influences on the upper atmosphere and ionosphere. Many important ionospheric phenomena have close relationship with the ionospheric electric fields. Incoherent Scatter Radar (ISR) and satellite are powerful tools to measure the ionosphere and electric field. Since 1970's, many authors have extensively investigated the electric fields by the ISR and satellites. Fejer *et al.*[1−3] published a series of paper on the F region electric field sounded by the Jicamarca ISR and AE-E satellite. Richmond *et al.*[4] used the $\boldsymbol{E} \times \boldsymbol{B}$ drifts observed over the four ISR stations (Arecibo, St. Santin, Millston Hill, and Jicamarca) in the middle of 1970s, to construct a seasonal averaged quiet-day empirical model for the electric fields. As a reference standard model, this model can provide the diurnal, longitude and latitude features of the electric fields in the low solar years, and was usually taken as input parameter in many ionospheric models.

Alternatively, computer simulation provides us

∗ Supported by National Natural Science Foundation of China (40974094, 41274159)

Received September 18, 2013. Revised March 03, 2014

E-mail: yutao@cma.gov.cn

ability to study the ionospheric electric fields and currents in a more general situation. With the thin shell model, Van Sabben[5] calculated the ionosphere currents. Tarpley[6−7] also calculated the ionospheric dynamo by this assumption, and investigated the influence of tide component on the current systems. Later, Untiedt[8], Sugiura and Poros[9] pointed out that the vertical currents must be included when studying the equatorial electrojet. Ignoring the longitudinal derivative $\partial/\partial\phi$, they constructed a two-dimension model in the meridional plane. However, these models need a zonal electric field to trigger and maintain the meridional currents, and their results were seriously dependence of that initial zonal electric field. As a result, three-dimension model is necessary in the study of electric fields, but the dynamo equations are too complex to derive fully three-dimension solutions.

With an assumption of the nearly infinite parallel conductivity and equipotential along the magnetic flux, Richmond[10−11] developed a three-dimension model to examine the physical features of the equatorial electrojet in detail. They found that the model currents and electric fields are relatively unaffected by assuming the parallel conductivity to be infinite. Thereafter, many authors tried to construct three-dimension models by assuming the infinite parallel conductivity. Takeda and Maeda[12] developed a three-dimension model of ionospheric electric fields, and successfully investigated the structure and morphology of the equatorial electrojet and currents in the meridional plane. Using an ionospheric model coupling with an electric fields model, Crain *et al.*[13] compared the influence of different neutral winds on the electric fields. An electric field model with the assumption of infinite parallel conductivity is introduced in this paper, which is the initial part of electrodynamics model of the Coupled Ionosphere and Thermospheric Model developed by Ren *et al.*[14−15]. As a preliminary result we introduce the development of the electric fields model in detail and its basic application.

1 Construction of the Dynamo Model

In the ionospheric dynamo region, the electrodynamics processes are controlled by the Maxwell equations. As for the slow-variation courses, the temporal variation terms in Maxwell equations can be ignored. Therefore the relation between the electric fields $\boldsymbol{E}$, currents $\boldsymbol{J}$, conductivity tensor $\boldsymbol{\sigma}$ and neutral wind velocity $\boldsymbol{W}$ can be described by the following dynamo equations.

$$\nabla \cdot \boldsymbol{J} = 0, \tag{1}$$

$$\boldsymbol{J} = \sigma_{//} E_{//} + \sigma_{\mathrm{p}}(E_{\perp} + \boldsymbol{W} \times \boldsymbol{B}) + \sigma_{\mathrm{H}} \boldsymbol{b} \times (E_{\perp} + \boldsymbol{W} \times \boldsymbol{B}), \tag{2}$$

$$\boldsymbol{E} = -\nabla U, \tag{3}$$

where U is electric potential corresponding to the electric field, $\sigma_{//}$, σ_{p}, σ_{H} are parallel, Pedersen and Hall conductivities, $\boldsymbol{b}$ is unit vector along geomagnetic field, $E_{//}$, $E_{\perp}$ are respectively the electric field components parallel and perpendicular to geomagnetic lines.

In this paper, the geomagnetic field is assumed to be a central dipole illustrated in Fig. 1, which is the same as the coordinate system introduced by Takeda and Maeda[12]. In the orthogonal coordinate system, t is downward and perpendicular to magnetic lines, s is poleward and align the geomagnetic lines. The third component ϕ is eastward and perpendicular to the meridional plane. We take the assumption that the magnetic lines are equipotential and the vertical current in the low boundary of the ionosphere is zero. Eqs. (2) and (3) are submitted to Eq. (1) and integrated along the flux lines, and the following equation suitable for calculation is derived as following.

$$A\frac{\partial^2 U}{\partial t^2} + B\frac{\partial^2 U}{\partial \phi^2} + D\frac{\partial U}{\partial t} + E\frac{\partial U}{\partial \phi} + F = 0, \tag{4}$$

where the coefficients are:

$$A = -\int_{S_1}^{S_2} \frac{h_s h_\phi \sigma_{\rm p}}{h_t} \cdot {\rm d}s,$$

$$B = -\int_{S_1}^{S_2} \frac{h_s h_t \sigma_{\rm p}}{h_\phi} \cdot {\rm d}s,$$

$$D = -\int_{S_1}^{S_2} \Big[\frac{\partial}{\partial t}\Big(\frac{h_s h_\phi \sigma_{\rm p}}{h_t}\Big) + \frac{\partial}{\partial \phi}(h_\phi \sigma_{\rm p})\Big] \cdot {\rm d}s,$$

$$E = -\int_{S_1}^{S_2} \Big[\frac{\partial}{\partial t}(h_\phi \sigma_{\rm p}) + \frac{\partial}{\partial \phi}\Big(\frac{h_s h_t \sigma_{\rm p}}{h_\phi}\Big)\Big] \cdot {\rm d}s,$$

$$F = \int_{S_1}^{S_2} \Big\{\frac{\partial}{\partial t}[-h_s h_\phi(\sigma_{\rm p} v B + \sigma_{\rm H} u B \sin I)] + \frac{\partial}{\partial \phi}[h_s h_t(\sigma_{\rm H} v B - \sigma_{\rm p} u B \sin I)]\Big\} \cdot {\rm d}s. \quad (5)$$

Here h_t, h_s, h_ϕ are geometrical scale factors of the dipolar geomagnetic field, which are adopted from Takeda and Maeda[12], u is the north component of the horizontal winds in the magnetic meridional plane, v is the east component horizontal wind perpendicular to meridional plane, I is the dip angle, S_1 and S_2 are the cross-points of the geomagnetic lines with the ionosphere lower boundary in the north and south hemispheres. Eq.(4) is the fundamental equation of the model. Given the boundary conditions (in this paper, the electric potential at boundary are derived from Weimer's model[16], Eq.(4) can be successfully solved by the line-by-line iteration method[17]. Thereafter, the electric potential, electric fields, and currents can be derived eventually.

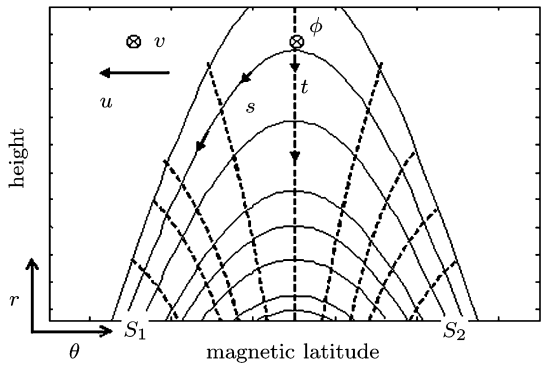


Fig. 1 Schematic diagram illustrates the relation between the coordinate systems of (t, s) and (r, θ), where r is the radial distance from the Earth center, θ is geomagnetic colatitude, t directs downward perpendicular to magnetic lines, s directs northward along geomagnetic lines, the third component ϕ is geomagnetic longitude which directs eastward and perpendicular to the meridional plane, u and v are the horizontal northward and eastward components of neutral wind

The neutral wind and the ionospheric conductivity are major parameters input into the model. We calculate the ion-neutral, ion-electron, and electron-neutral collision frequencies from the formulas of Richmond[18], and then calculate the ionospheric conductivity by the formulas of Forbes[19]. Moreover, the empirical models IRI90 and MSISE90 are used to provide the concentrations and temperatures of electron, ions and neutrals. Fig. 2 shows the altitude profiles of night (dashed) and noon (solid) Pedersen and Hall conductivities at the magnetic equator. The neutral wind is directly taken from the horizontal wind model HWM93, which can roughly reproduce the global F region thermospheric and E region tidal.

2 Results and Discussions

Preliminary results are presented in this section to illustrate the validity and reliability of our model. In the following calculation, if there's no special statement, we take the solar 10.7 cm flux index $F_{10.7} = 75$, which indicates the low solar activity condition, and the geomagnetic index $Ap = 6.0$, the calculated date

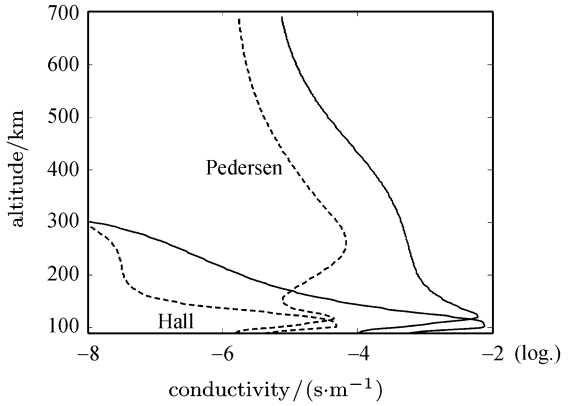


Fig. 2 Altitude profiles of night (dashed) and noon (solid) Pedersen and Hall conductivities in the magnetic equator ionosphere. Here $F_{10.7} = 75$

is fixed on March Equinox, the height ranges from 90 km to 700 km, and the latitude extends from magnetic 60°S to 60°N.

2.1 Calculated Electric Fields

Being indispensable input parameter for many ionospheric models, the vertical drift (corresponding to the zonal electric field) has significant influence on the plasma distribution in the mid-and low-latitude ionosphere. Since the input parameters, such as the wind and conductivity, are roughly calculated from the external empirical models, it is not expected that close agreement with the observation would result. Rather, the general structure and morphology of the model electric fields are most concerned in the following discussion.

Fig. 3 shows the calculated vertical (Panel a) and zonal (Panel b) electric fields at the height of 300 km over 0° longitude sector, which is about the same sector as observations included in Richmond's empirical model. It may be seen from the Fig. 3(a) that the calculated vertical electric field (solid line) is favorably comparable to Richmond's empirical mode result (plus sign). In general, the vertical electric field is upward with a magnitude of $-1\,\mathrm{mV\cdot m^{-1}}$ or so and reaches its maximum at 14:00 LT, and downward with a magnitude of over $4\,\mathrm{mV\cdot m^{-1}}$ and peaks at 20:00 LT. It is obvious that the dawn and dusk reversal time of the vertical electric field is well agreeable in both models, and only some discrepancies remain in the daytime and earlier evening. Whereas, from Fig. 3(b), the zonal electric field derived from our model and the empirical model does not fit so well. In daytime, the zonal electric field is eastward with an average magnitude of about 0.5 mV. At night, the zonal field is slightly larger but in the opposite direction. It should be noticed that dramatic discrepancies between our model and the empirical one are obvious during the period of earlier morning and earlier evening. In the earlier morning (04:00 LT), our model eastward electric field has an obvious negative decline, which is infrequently observed in the low solar activity years and usually excluded by empirical model. This negative decline was also reproduced by Crain's *et al.*[13] calculation, and was successfully eliminated when they coupled calculated their electric field model with an ionospheric model. Moreover, the evening prereversal enhancement (18:00 LT), generally observed throughout the solar maximum year, is still prominent in our simulation for the solar minimum condition. We suggest that these discrepancies may be partly due to the inaccuracy of the external model.

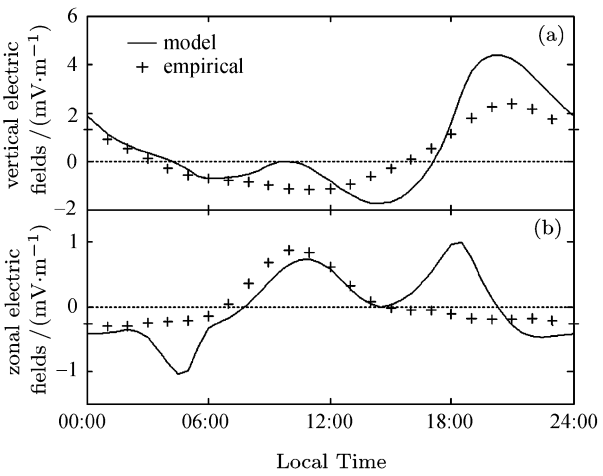


Fig. 3 Diurnal variations of the vertical and zonal electric fields at the height of 300 km in the magnetic equatorial ionosphere. The positive sign correspond to downward in (a) and eastward in (b), respectively

2.2 Solar and Magnetic Latitude Variations

Many ionospheric phenomena have strong dependence on the solar activity, so does the electric field, and major feature between the solar activity and the electric fields have been studied by previous authors, Woodman *et al.*[20] and Fejer *et al.*[1] studied the solar dependence of electric fields with the observation data. With Thermosphere/Ionosphere/Electrodynamic General Circulation Model (TIEGCM) provided by the National Center for Atmospheric Research, Fesen *et al.*[21] successfully simulated the solar cycle dependence of the quiet-time F region plasma drifts. In the following, we respectively calculate the electric fields in the solar maximum (dash line) and minimum (solid line) to get a glimpse of the solar variation of the model electric field. As illustrated in Fig. 4, the strength of

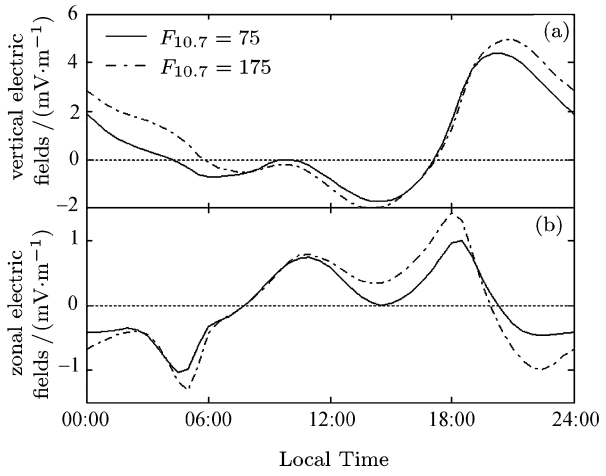


Fig. 4 Solar dependence of the vertical and the zonal electric fields at the height of 300 km in the magnetic equatorial ionosphere. The dash line indicates the solar maximum case and the solid line indicates the solar minimum case, respectively. The positive sign correspond to downward in (a) and eastward in (b) respectively

the electric fields are remarkably influenced by the solar $F_{10.7}$ flux during the period of later afternoon and night, and less influenced during the period of morning and noon. The details can be summarized as follows. (1) The zonal electric field generally seems to be in weak independence on the solar activity in the morning but strong solar-dependence in the afternoon and evening, and it is large at solar maximum and small at the minimum. (2) The evening pre-reversal enhancement of the zonal electric filed is very prominent in the solar maximum and rather weak in the solar minimum. (3) The nighttime vertical electric field depends also on the solar activity, and the nighttime electric field is large at solar maximum and small at solar minimum.

In our model, the boundary latitude can extend up to 60° along the geomagnetic lines, so we can investigate the latitudinal variation of the model electric fields. Fig. 5 shows contour of the vertical (a) and zonal (b) electric fields versus the magnetic latitude and local time. It is clear that both the vertical and zonal electric fields are well symmetric with the magnetic equator, and we attribute this symmetry to the assumption of nearly infinite parallel conductivity. Moreover, the calculated date is at equinox when

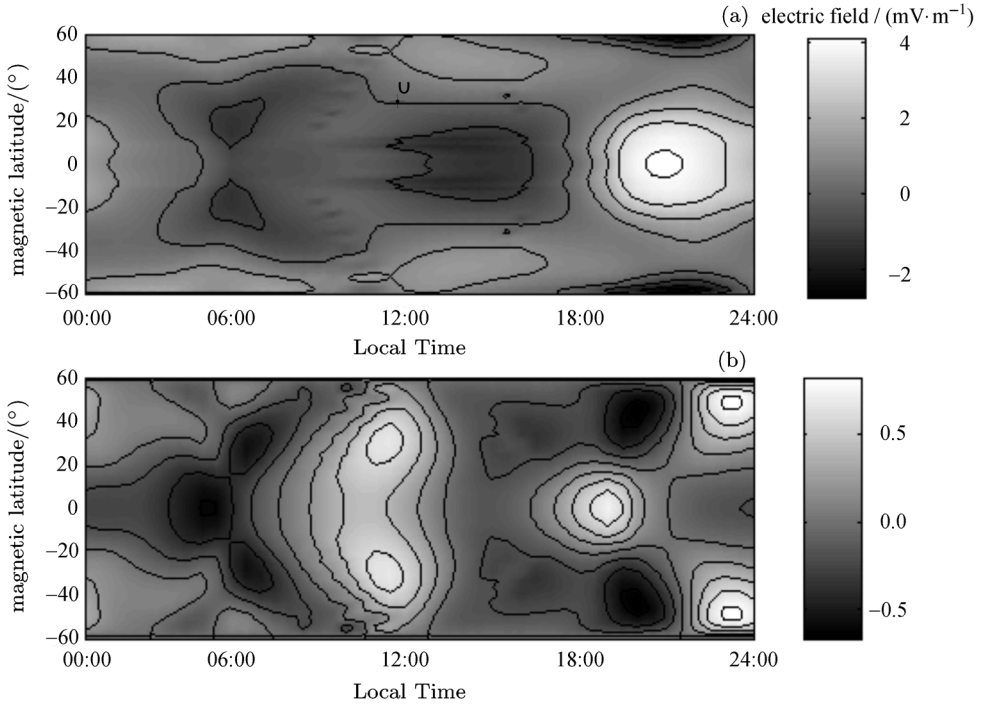


Fig. 5 Contour of the vertical (a) and zonal (b) electric fields versus the magnetic latitude and local time at the height of 300 km

the ionosphere is also well symmetric. As shown in Fig. 5(b), the zonal electric field seem to be significant gradient along the latitude during the evening pre-reversal enhancement period (18:00 LT−20:00 LT), which indicate that the evening pre-reversal enhancement is pronounced at the magnetic equator and nearly absent at the magnetic latitude of 20° and even negative at the magnetic latitude of 40°. As shown in Fig. 5(b), the morning enhancement (10:00 LT−12:00 LT) of zonal electric fields, which is regard as the E region dynamo action and controlled by the solar radiation[22], is not strongly dependent on the magnetic latitude. The morning enhancement of zonal electric fields peaks at magnetic latitude of 30°, and within the magnetic latitude of ±40°, it has few gradient along the magnetic latitudinal direction, it is interesting that the morning enhancement of electric fields seems to be similar with the electron concentration hump.

3 Further Discussion

Being the most important input parameters, the neutral wind and the conductivity, have significant influence on the calculated results. But lacking of observed data, we have to take the HWM 93 to get the neutral winds, and the IRI 90 to get the electron concentration, the temperature to calculate the conductivity. However, there would be much inaccuracy and impropriety from those external empirical models, which would lead to the inaccuracy and discrepancy of the calculated electric fields. In the following we would investigate how much the wind and conductivity can influence our model electric fields, and try to give some possible reason to those discrepancies in detail.

3.1 Influence of Tide Dynamo

It is generally accepted that the E region tidal winds drag the plasmas across the magnetic flux, and the electron and ions are separated in opposite direction due to the difference between their ratios of collision frequencies to gyromagnetic frequencies, so that the currents and the electric fields appear. This process, called E region dynamo action, is predominant in the daytime, while the F region dynamo action should be considered at nighttime[13,23] . Moreover, the diurnal and semidiurnal components of the tide wind are proved to be the most effective source to drive the E region dynamo in daytime. However, those two tide components have different contribution to the electric fields. If just used the HWM90 model input wind, Du *et al.*[22] failed to reproduce the observed electric fields, and they attributed their failures to that either the semidiurnal component is too strong or the diurnal component is too weak.

In Fig. 6 we compare the influence of the diurnal and semidiurnal components of tide wind in the HWM93 model on the electric fields. In order to discuss how far each component can influence the electric fields, we calculated the electric fields in the following cases: (1) no diurnal component (when run our model, we remove the diurnal component from the HWM93 wind); (2) no semidiurnal component; (3) no diurnal and no semidiurnal components. As shown in Fig. 6 the results reveal that both the diurnal and the

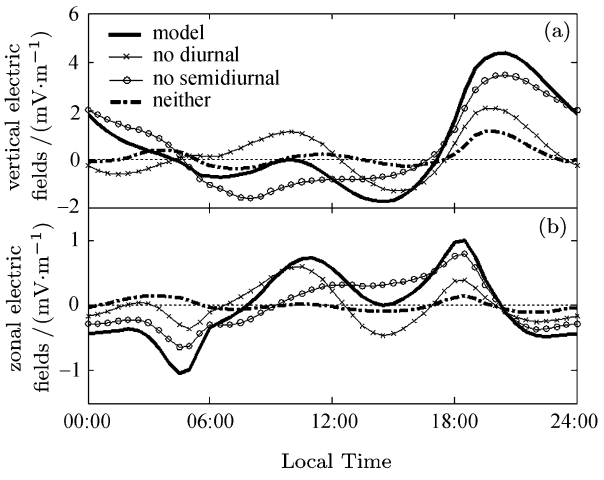


Fig. 6 Influence of diurnal and semidiurnal tide components on the vertical (a) and the zonal (b) electric fields at the height of 300 km in equatorial ionosphere. The positive sign corresponds to downward in (a) and eastward in (b), respectively

semidiurnal components do play essential roles on electric fields. The winds without diurnal tide can reproduce the major form of the zonal electric field (Panel b), but fail to reproduce the vertical electric field (Panel a). On the other hand, the winds removing the semidiurnal tide can well reproduce the general form of the vertical electric field, but fail to reproduce the zonal electric field. If we entirely remove the diurnal and semidiurnal tides, it may be found that the amplitudes of both electric fields are greatly depressed, and their general morphology is also changed. But, the evening pre-reversal of zonal electric field is still visible while with much smaller amplitude. From the above discussion, we may draw the following conclusion. (1) The diurnal and semidiurnal tides play important roles in the formation of the electric fields, especially to their strengths in daytime. (2) The diurnal tide has significant contribution to the vertical electric field and the semidiurnal tide has important contribution to the zonal electric field. (3) The evening pre-reversal phenomena did not entirely vanish even both components of the tides are removed and it may be controlled by other physics process.

3.2 Influence of F Region Dynamo

Many authors have proposed the evening pre-reversal of zonal electric field be mainly due to the F region dynamo action, which is reinforced by the rapid diminution of E region conductivity and slow decreasing of F region conductivity, as well as the strong wind during that period[13,24]. Fig. 7 illustrates the diurnal variations of the Pederson conductivities in the E and F region respectively, it seems that the Pederson conductivity varied quite consistent with the solar zenith angle in the E region, but quite different in the F region. The Pederson conductivity had decreased to a very small magnitude after sunset in E region, whereas it maintained as a very high magnitude until late night. In the same time, the simulation results in Fig. 8 confirm that F region dynamo mainly contributed the zonal electric fields at night, as well as the discrepancies of the Pederson conductivity in E region and F region maybe the most probably contribution to the evening pre-reversal of zonal electric field.

In the following we will respectively adjust the F region winds and the F region conductivity at the pre-reversal time, so as to investigate their contributions to this phenomenon, and improve the agreement between the calculated and empirical model electric fields.

During the period of sunrise and sunset, there is great discrepancy between our model and the empirical model, for simplicity, we just reduce the winds to half of their original amplitudes during those periods. As shown in Fig. 9, the electric fields produced by the modified winds do have marked change during those

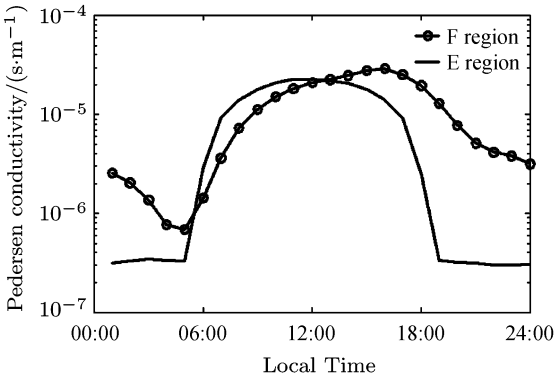


Fig. 7 Diurnal variation for the Pedersen conductivities in the E region (solid line) and F region (solid line with circles)

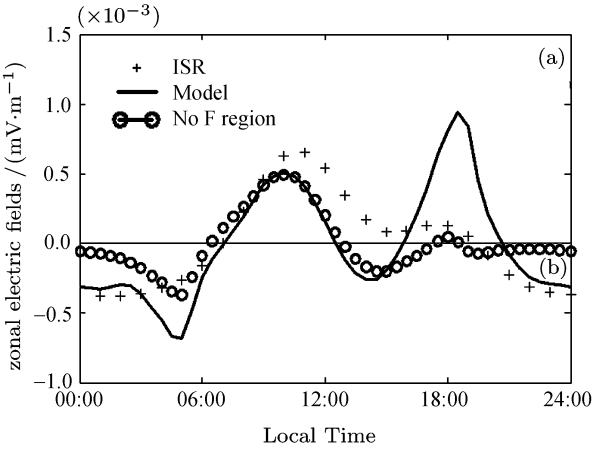


Fig. 8 Diurnal variation for zonal electric fields with (solid line) and without (circles) F region dynamo

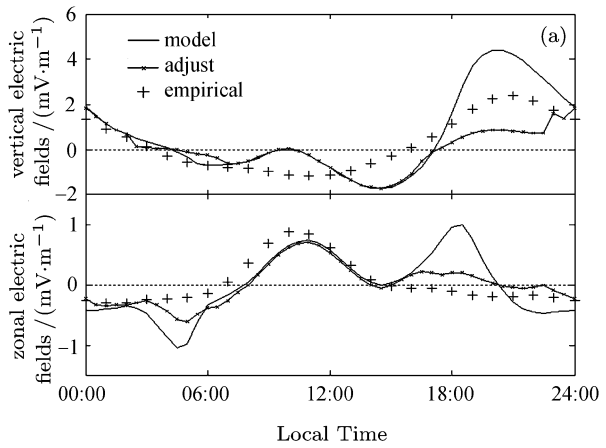


Fig. 9 Vertical (a) and zonal (b) electric fields at 300 km of equatorial ionosphere after reducing the wind to half of the original amplitude. The positive sign correspond to downward in (a) and eastward in (b), respectively

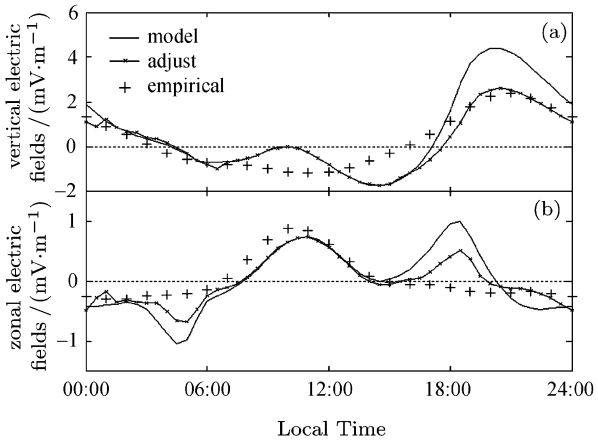


Fig. 10 Vertical (a) and zonal (b) electric fields at 300 km of equatorial ionosphere after adjusting of the F region conductivity. The positive sign correspond to downward in (a) and eastward in (b), respectively

periods. In Fig.9(b), the noticeable evening pre-reversal of the zonal electric field is effectively smooth out and the calculated zonal electric field fit closely with the empirical model, and it is the same story in the earlier morning. In Fig.9(a), the vertical electric fields also have marked change during those periods. In view of these results, we may conclude that the F region winds do play essential role in the formation of the electric fields during these periods, and the difference between our model and the empirical model are mainly due to the input HWM93 winds.

To study the influence of F region conductivity on the electric fields, we quickly decrease the F region conductivity after sunset and slowly decrease it before sunrise than the previous calculation, the results displayed in Fig. 10 show that adjusting of the F region conductivity can depress the evening pre-reversal enhancement of electric fields to some extent and eliminate the discrepancy between our model and the empirical one, but it is not as effective as the wind-adjusting shown in Fig. 9. Therefore, we are convinced that the difference of the E and F regions conductivity does have some contributions to the sharp increase for the zonal electric field before sunrise and after sunset.

4 Conclusion

A theoretical model for mid-and low-latitude ionospheric electric field and its application is presented in this paper. Major work is briefly recapitulated as follows.

(1) Based on the ionosphere dynamo theory, a theoretical model for ionospheric electric fields at mid-and low-Latitudes is established. The conductivity is determined by the theoretical formulas of Forbes (1981). The neutral wind is calculated by empirical model HWM 93.

(2) With the ionospheric electric model, we investigate the solar activity and magnetic latitude variations of the calculated electric fields at the height of 300 km, and find their tendency of variation is similar with previous work as well as the empirical model. Moreover, we study the influence of the diurnal and semidiurnal components of tide wind on the electric fields, and find that the diurnal tide is mainly contributed to the formation of the vertical electric field, while the semidiurnal tide mainly contributed to the zonal electric field.

(3) By adjusting the input wind or conductivity in the F region, we can eliminate the earlier morning and evening pre-reversal enhancements of the zonal

electric field calculated from our model. We confirm that the F region dynamo also plays an important role in the electric dynamics process during the sunrise and sunset periods, especially to the formation of the zonal electric field pre-reverse enhancement.

References

[1] Fejer B G, D T Farley, R F Woodman, *et al.* Dependence of equatorial F region vertical drifts on season and solar circle [J]. *J. Geophys. Res.*, 1979, **84**:5792

[2] Fejer B G. The equatorial ionospheric electric fields—A review [J]. *J. Atmos. Terr. Phys.*, 1981, **43**:377

[3] Fejer B G, E R de Paula, R A Heelis, *et al.* Global equatorial ionospheric vertical plasma drift measured by the AE-E satellite [J]. *J. Geophys. Res.*, 1995, **100**:5769

[4] Richmond A D, M Blanc, B A Emery, *et al.* An empirical model of quiet- day ionospheric electric fields at middle and low latitudes [J]. *J. Geophys. Res.*, 1980, **85**:4658

[5] Van Sabben D. Ionospheric current systems caused by non-periodic winds [J]. *J. Atmos. Terr. Phys.*, 1962, **24**:959-974

[6] Tarpley J D. The ionospheric wind dynamo-I, Lunar tide [J]. *Planet. Space Sci.*, 1970, **18**:1075

[7] Tarpley J D. The ionospheric wind dynamo-II, Solar tide [J]. *Planet. Space Sci.*, 1970, **18**:1090

[8] Untiedt J. A model of the equatorial electrojet involving meridional currents [J]. *J. Geophys. Res.*, 1967, **72**:5779

[9] Sugiura M, Poros D J. An improved model equatorial electrojet with a meridional current system [J]. *J. Geophys. Res.*, 1969, **74**:4025

[10] Richmond A D. Equatorial electrojet-I. Development of a model including winds and instabilities [J]. *J. Atmos. Terr. Phys.*, 1973, **35**:1083

[11] Richmond A D. Equatorial electrojet-II. Use of the model to study the equatorial ionosphere [J]. *J. Atmos. Terr. Phys.*, 1973, **35**:1105

[12] Masahiko T, Taeda H. Three-dimensional structure of ionospheric currents, I, currents caused by diurnal tidal winds [J]. *J. Geophys. Res.*, 1980, **85**:6895

[13] Crain D J, Heelis R A, Bailey G J, *et al.* Low-latitude plasma drift from a simulation of the global atmospheric dynamo [J]. *J. Geophys. Res.*, 1993, **98**:6039

[14] Ren Z P, Wan W X, Wei Y, *et al.* A theoretical model for mid-and low-latitude ionospheric electric fields in realistic geomagnetic fields [J]. *Chin. Sci. Bull.*, 2008, **53**(24):3883

[15] Ren Z P, Wan W X, Liu L B. GCITEM-IGGCAS: A new global coupled ionosphere-thermosphere-electrodynamics model [J]. *J. Atmos. Terr. Phys.*, 2009, **71**:2064

[16] Weimer D R. A flexible IMF dependent model of high-latitude electric potentials having space weather applications [J]. *Geophys. Res. Lett.*, 1996, **23**:2549

[17] Hu Y Q, Wu S T. A Full-Implicit-Continuous-Eulerian (FICE) scheme for multidimensional transient magnetohydrodynamic (MHD) flows [J]. *J. Comput. Phys.*, 1984, **55**:33

[18] Richmond A D. Numerical model of the equatorial electrical electrojet. *Rep. AFCRL-72-0668, ERP 421*, Air Force Cambridge Res. Lab., Hanscom AFB, Bedford, Mass. 1972

[19] Forbes J. The equatorial electrojet [J]. *Rev. Geophys. Space Phys.*, 1981, **19**:469

[20] Woodman R F, Rastongi R G, Calderon C. Solar cycle effects on the electric fields in the equatorial ionosphere [J]. *J. Geophys. Res.*, 1977, **82**:5257

[21] Fesen C G, Crowley G, Roble R G, *et al.* Simulation of the pre-reversal enhancement in the low latitude vertical ion drifts [J]. *Geophys. Res. Lett.*, 2000, **27**:1851

[22] Du J, Stening R J . Simulating the ionospheric dynamo-II. Equatorial electric fields [J]. *J. Atmos. Terr. Phys.*, 1999, **61**:925

[23] Rishbeth H. The F-layer dynamo [J]. *Planet. Space Sci.*, 1971, **19**:263

[24] Farley D T, E Bonelli, B G Fejer, *et al.* The pre-reversal enhancement of the zonal electric field in the equatorial ionosphere [J]. *J. Geophys. Res.*, 1986, **91**:13 723